**Title:** Human white adipose tissue vasculature contains endothelial colony-forming cells with robust in vivo vasculogenic potential

**Short title:** Endothelial colony-forming cells in adipose tissue

**Authors and Affiliations**

* Ruei-Zeng Lin [1], * Rafael Moreno-Luna [1,2], Rocío Muñoz-Hernandez [2], Dan Li [3], Shou-Ching S. Jaminet [3], Arin K. Greene [4], and Juan M. Melero-Martin [1]

[1] Department of Cardiac Surgery, Boston Children's Hospital, Harvard Medical School, Boston, MA.

[2] Unidad Clínico-Experimental de Riesgo Vascular (UCAMI-UCERV), Servicio de Medicina Interna, Hospital Universitario Virgen del Rocío, and Instituto de Biomedicina de Sevilla (IBiS), Seville, Spain.

[3] Center for Vascular Biology, Department of Pathology, Beth Israel Deaconess Medical Center, Harvard Medical School, Boston, MA.

[4] Department of Plastic & Oral Surgery, Boston Children's Hospital, Harvard Medical School, Boston, MA.

* R.-Z.L. and R.M.-L. contributed equally to this study.

**Corresponding Author:**

Dr. Juan M. Melero-Martin

Department of Cardiac Surgery

Boston Children's Hospital

300 Longwood Ave., Enders 349

Boston, MA 02115

Tel.: (617) 919-3072

Fax: (617) 730-0235

Email: **juan.meleromartin@childrens.harvard.edu**

**Keywords:** endothelial colony-forming cells; endothelial progenitor cells; adipose tissue; peripheral blood; vasculogenesis

**Abstract**

Blood-derived endothelial colony-forming cells (ECFCs) have robust vasculogenic potential that can be exploited to bioengineer long-lasting human vascular networks in vivo. However, circulating ECFCs are exceedingly rare in adult peripheral blood. Because the mechanism by which ECFCs are mobilized into circulation is currently unknown, the reliability of peripheral blood as a clinical source of ECFCs remains a concern. Thus, there is a need to find alternative sources of autologous ECFCs. Here we aimed to determine whether ECFCs reside in the vasculature of human white adipose tissue (WAT) and to evaluate if WAT-derived ECFCs (watECFCs) have equal clinical potential to blood-derived ECFCs. We isolated the complete endothelial cell (EC) population from intact biopsies of normal human subcutaneous WAT by enzymatic digestion and selection of $CD31^+$ cells. Subsequently, we extensively compared WAT-derived EC phenotype and functionality to bonafide ECFCs derived from both umbilical cord blood and adult peripheral blood. We demonstrated that human WAT is indeed a dependable source of ECFCs with indistinguishable properties to adult peripheral blood ECFCs, including hierarchical clonogenic ability, large expansion potential, stable endothelial phenotype, and robust in vivo blood vessel-forming capacity. Considering the unreliability and low rate of occurrence of ECFCs in adult blood and that biopsies of WAT can be obtained with minimal intervention in an ambulatory setting, our results indicate WAT as a more practical alternative to obtain large amounts of readily available autologous ECFCs for future vascular cell therapies.

## Introduction

Future vascular cell therapies and tissue engineering applications will likely rely on having a robust, clinically suitable source of autologous endothelial cells (ECs). The discovery of highly proliferative endothelial colony-forming cells (ECFCs) in human peripheral blood created a promising opportunity to non-invasively obtain large quantities of readily available ECs [1-3]. Indeed, studies have shown that blood-derived ECFCs have robust vasculogenic potential that can be exploited to bioengineer long-lasting, functional human vascular networks in vivo [3-7].

However, it is well recognized that while ECFCs are abundant in umbilical cord blood (cbECFCs), they are exceedingly rare in adult peripheral blood (pbECFCs) [2,8,9]. Yoder et al. estimated the frequency of pbECFC colonies as 0.017 per million blood mononuclear cells (MNC) in healthy adults, which is approximately 15-fold lower than in umbilical cord blood [9]. This low occurrence has created uncertainty around adult peripheral blood as a source of ECs. In fact, there are increasingly more studies recognizing absence of pbECFCs in a substantial proportion (27-31%) of healthy adult subjects [10-12]. This apparent lack of pbECFCs has also been described in non-healthy subjects, including patients with coronary artery disease (46%) [11] and age-related macular degeneration (28%) [12]. Currently, the mechanism by which pbECFCs are mobilized into circulation, and how this process is modulated with age, in health and disease, is completely unknown; thus the reliability of peripheral blood as a source of ECFCs remains a concern.

For decades, harvesting ECs from healthy blood vessels has been largely dismissed as an option with broad clinical future because, apart from creating site morbidity, “mature” ECs were thought to have limited replicative capacity. However, studies have shown that ECs derived from the wall of some blood vessels can achieve a significant number of population doublings in culture (30-40 PD), including those isolated from the umbilical vein, aorta, carotid artery, and

skin microvasculature [13,14]. This replicative capacity is similar to that reported for circulating pbECFCs [2,3,15]. Moreover, Ingram et al. demonstrated that both the aorta and the umbilical vein contain a complete hierarchy of highly proliferative ECs with equal colony-forming ability to blood-derived ECFCs [16], which suggested the actual vascular wall as a possible source of circulating ECFCs [17]. Whether ECFCs reside in the vasculature of all human tissues remains uncertain. Certainly, ECs can be obtained from tissues such as white adipose tissue (WAT) [18,19], but whether these ECs have similar clinical potential to blood-derived ECFCs has not been rigorously determined. Here, we examined the potential of human subcutaneous WAT as a source of ECFCs and compared it to both umbilical cord and adult peripheral blood.

## Methods

### Isolation of ECFCs and MSCs from WAT

Normal discarded subcutaneous WAT samples (n=5) were obtained during a clinically-indicated procedure in accordance with an Institutional Review Board-approved protocol. WAT samples were washed, minced and enzymatically (collagenase and dispase) digested for 1h at 37°C. The stromal vascular fraction (SVF) was obtained after removal of mature adipocytes by centrifugation (450xg for 10 min) and the lysis of erythrocytes with ammonium chloride solution [20]. watECFCs were purified by magnetic activated cell sorting (MACS) using CD31-coated magnetic beads (Dynalbeads; Invitrogen, Grand Island, NY). CD31-selected WAT-derived ECFCs (referred to as watECFCs) were cultured on 1% gelatin-coated plates using ECFC-medium: EGM-2 (except for hydrocortisone; Lonza, Walkersville, MD) supplemented with 20% FBS, 1x glutamine-penicillin-streptomycin (GPS; Invitrogen, Carlsbad, CA). WAT-derived mesenchymal stem cells (MSCs) (referred to as watMSCs) were obtained from the $CD31^-$ cell fraction of the SVF and were cultured onto non-coated plates using MSC-medium: MSCGM Mesenchymal Stem Cell Medium BulletKit (basal media and SingleQuots; Lonza),

supplemented with 10 % FBS, 1xGPS, and 10 ng/mL of FGF-2 (R&D Systems, Minneapolis, MN). Human ECFCs were isolated from both umbilical cord blood (cbECFCs) and adult peripheral blood (pbECFCs), as previously described [4]. Human MSCs were isolated from bone marrow aspirates (bmMSCs), as previously described [4].

**Expansion potential of watECFCs**

watECFCs were expanded for 50 days. All passages were performed by plating the cells onto 1% gelatin-coated tissue culture plates at $5x10^3$ cell/$cm^2$ using ECFC-medium. Medium was refreshed every 2 to 3 days and cells were harvested by trypsinization and replated in the same culture conditions for the next passage. Cumulative values of total cell number were calculated by counting the cells at the end of each passage using a hemocytometer.

**Endothelial colony-forming assay**

For Passage 2 (P2) ECFCs were culture for 10 days at clonal density (200 cell/60 $cm^2$; 600 cells plated; n=3 per ECFC type) onto 1% gelatin-coated plates using ECFC-medium. Medium was refreshed every 4 days. At day 10, colonies containing 8 or more cells (i.e., at least 3 divisions) were scored under a fluorescence microscope after DAPI staining of the nuclei. Endothelial phenotype was confirmed by binding of rhodamine-labeled *Ulex Europaeus Agglutinin I* (UEA-1; 1:100; Vector Laboratories, Burlingame, CA) using a fluorescent microscope. Colonies were categorized into large (>300 cells), medium (100-300 cells) and small (8-100 cells) size. The number of cells in each colony was quantified under a fluorescent microscope after DAPI staining using ImageJ analysis software (NIH, Bethesda, MD, USA).

**Phenotypical and functional characterization of ECFCs and watMSCs**

The rest of the phenotypic and functional assays that were used to characterize watECFCs and watMSCs in vitro are detailed in the online Supplemental Methods.

**in vivo vasculogenic assay**

Six-week-old athymic nu/nu mice were purchased from Massachusetts General Hospital (Boston, MA). Mice were housed in compliance with Boston Children's Hospital guidelines, and all animal-related protocols were approved by the Institutional Animal Care and Use Committee. Vasculogenesis was evaluated in vivo using our xenograft model as previously described [21]. Briefly, ECFCs and MSCs ($2x10^6$ total; 2:3 ECFC/MSC ratio) were resuspended in 200 µl of collagen/fibrin–based solution (3 mg/mL of bovine collagen, 30 ug/mL of human fibronectin, 25mM HEPES, 10% 10x DMEM, 10% FBS, and 3 mg/mL of fibrinogen, pH neutral). Before cell injection, 50 uL of 10 U/mL thrombin was subcutaneously injected. All experiments were carried out in 4 mice.

**Histology and immunohistochemistry**

Implants were removed from euthanized mice, fixed in 10% buffered formalin overnight, embedded in paraffin, and sectioned (7-µm-thick). Hematoxylin and eosin (H&E) stained sections were examined for the presence of blood vessels containing red blood cells. For immunohistochemistry, sections were deparaffinized, and antigen retrieval was carried out by heating the sections in Tris-EDTA buffer (10 mM Tris-Base, 2 mM EDTA, 0.05% Tween-20, pH 9.0). The sections were blocked for 30 min in 5-10% blocking serum and incubated with primary antibodies for 1h at RT. The following primary antibodies were used: mouse anti-human CD31 (1:50; DakoCytomation, M0823 Clone JC70A), mouse anti-human α-smooth muscle actin (α-SMA; 1:200; Sigma-Aldrich, A2547 Clone 1A4), and mouse IgG (1:50; DakoCytomation). Horseradish peroxidase-conjugated mouse secondary antibody (1:200; Vector Laboratories) and 3,3'-diaminobenzidine (DAB) were used for detection of hCD31, followed by hematoxilin counterstaining and Permount mounting. Fluorescent staining were performed using rhodamine-

conjugated UEA-1 (20 µg/mL) and FITC-conjugated secondary antibodies (1:200; Vector Laboratories) followed by DAPI counterstaining.

**Microvessel density**

Microvessel density was reported as the average number of erythrocyte-filled vessels (vessels/$mm^2$) in sections from the middle of the implants as previously described [3]. The entire area of each section was analyzed. Values reported for each experimental condition correspond to mean ± S.D. obtained from four individual mice.

**Quantification of lumenal engraftment of ECFCs**

Rhodamine-conjugated UEA-1 (100 uL; 1 mg/mL in normal saline) was intravenously injected into the tail vein of implant-bearing mice 10 min before harvesting the implants at day 8. Implants were removed from euthanized mice, enzymatically (collagenase and dispase) digested for 1 h at 37°C, and the retrieved cells analyzed by flow cytometry (FC) after incubation with PerCP-conjugated anti-mouse CD45 (1:100; BD Biosciences), APC-conjugated anti-human CD90 (1:100; BD Biosciences), and FITC-conjugated anti-human CD31 antibodies (1:100; BD Biosciences). ECFCs in each implant were identified as $mCD45^-/hCD31^+$ cells. Perfused ECFCs were identified as $mCD45^-/hCD31^+/UEA\text{-}1^+$ cells.

**Statistical analysis**

Data were expressed as mean ± S.D. Comparisons between groups were performed by ANOVA followed by Tukey's multiple post-test analysis using Prism Version 4 software (GraphPad). $P<0.05$ was considered statistically significant.

## Results

### Human WAT is a dependable source of proliferative ECFCs

Small biopsies of WAT can be obtained with minimal intervention, without liposuction, in an ambulatory, office-based setting. To reproduce this prospective way of sampling, intact specimens of normal subcutaneous WAT (1 g) were surgically excised with minimal tissue disruption. WAT samples were then minced, enzymatically digested and the SVF obtained (Figure 1A). Using CD31-coated magnetic beads, ECs were separated (refereed to as watECFCs) and grew up as colonies after one week in culture (Figure 1B). EC colonies were left to merge and grow until confluence (Figure 1C) and were then routinely subcultured. This methodology was reliable and watECFCs were isolated in all WAT samples processed (5/5). watECFCs were serially passaged (up to P7) to determine their expansion potential. We obtained $10^8$ watECFCs in approximately 25 days (P3) and as much as $4x10^9$ watECFCs in 40 days (P6) (Figure 1D).

The presence of highly proliferative, colony-forming cells was examined at clonal density (200 cells/60 $cm^2$). This evaluation was carried out at P2 to avoid excessive culture-mediated selection of highly proliferative cells. We found that 7% of watECFCs gave rise to visible independent colonies (>3 cell divisions), which was significantly lower than in cbECFCs (16%) and pbECFCs (15%) (Figure 1F). watECFCs had a hierarchical distribution of cells with different clonal proliferative ability (Figure 1G), which is consistent with previous observations on blood-derived ECFCs [2]. The percentage of medium-size (100-300 cells) colonies was significantly higher in pbECFCs (8%) than in watECFCs (2%). However, the percentage of highly-proliferative (>300 cells) colonies was statistically similar ($p>0.05$) in cbECFCs (2.3%), pbECFCs (0.3%), and watECFCs (0.1%). Taken together, we demonstrated that WAT is a particularly dependable source of ECFCs with hierarchical clonogenic ability.

**Robust endothelial phenotype of watECFCs**

To ensure bonafide endothelial phenotype, we extensively interrogated cells in culture (Figure 2 and online Supplemental Figure 1). All watECFCs displayed typical cobblestone-like morphology and expressed the EC markers CD31 and VE-cadherin in cell-cell borders and von Willebrand factor (vWF) in a punctuate pattern in the cytoplasm (Figure 2A). With respect to purity, FC showed uniform expression of CD31 (>96%) as well as negligible presence of either mesenchymal ($CD90^+$) or hematopoietic ($CD45^+$) cells (Figure 2B). The positive expression of EC markers and lack of mesenchymal markers was confirmed by qRT-PCR: all three ECFCs (cbECFCs, pbECFCs, watECFCs) had abundant mRNA copies for CD31, vWF, VE-Cadherin, VEGFR-2, and eNOS (normalized to 18S rRNA abundance), but not for CD90 and PDGFR-β (Figure 2C). Human mesenchymal stem cells (MSCs) from both bone marrow and WAT (referred to as bmMSCs and watMSCs) served as non-endothelial controls. Additionally, as expected for human ECs, watECFCs showed specific affinity for the binding of UEA-1 lectin to their surface (Figure 2D) and for uptake of acetylated low density lipoproteins (Ac-LDL) (Figure 2E).

The characterization of watECFCs was extended to several assays that confirmed endothelial functionality in vitro. watECFCs were responsive (proliferation and migration) to VEGF-A (10 ng/mL) and FGF-2 (1 ng/mL), and there were no significant difference between watECFCs, pbECFC, and cbECFCs in their response towards these angiogenic factors (Figure 3A-B). watECFCs were also able to assemble into capillary-like structures onto Matrigel (Figure 3C), and the extent of tube formation was statistically similar to both pbECFCs and cbECFCs. Finally, watECFCs were able to up-regulate the expression of leukocyte adhesion molecules (E-selectin, ICAM-1) upon exposure to the inflammatory cytokine tumor necrosis factor-alpha (TNF-α; 10 ng/mL), which resulted in a subsequent increase in leukocyte binding (Figure 3D-E).

The capacity to up-regulate leukocyte adhesion molecules was present in all three ECFC groups (Figure 3D-E and online Supplemental Figure 1), although more leukocytes bound cbECFCs and pbECFCs than watECFCs after TNF-α stimulation. Collectively, this exhaustive characterization revealed that (1) watECFCs were undoubtedly ECs, and (2) WAT- and blood-derived ECFCs are phenotypically highly similar.

**Modulation of MSC smooth muscle differentiation**

Another property of bonafide ECs is the capacity to modulate MSC differentiation into vascular smooth muscle cells (SMCs). To test whether watECFCs had this capacity, we isolated WAT-resident MSCs (referred to as watMSCs) from the same WAT biopsies from which we obtained watECFCs; watMSCs were grown from the $CD31^-$ cell fraction that resulted from the MACS procedure used to isolated $CD31^+$ watECFCs (Supplemental Figure 2). watMSCs were grown until 80% confluence and then routinely passaged. In culture, watMSCs displayed a characteristic spindle-shape morphology in culture and were highly homogenous with regards to cell surface markers expression: FC showed uniform expression of mesenchymal marker CD90 (>97%) as well as negligible presence of either endothelial ($CD31^+$) or hematopoietic ($CD45^+$) cells (Supplemental Figure 2). The MSC phenotype was confirmed by the ability of watMSCs to differentiate into cells from multiple mesenchymal lineages [22]. watMSCs differentiated into adipocytes, osteocytes and chondrocytes, as shown by the intracellular accumulation of oil droplets (adipogenesis), calcium deposition (osteogenesis) and glycosaminoglycan deposition in pellet cultures (chondrogenesis), respectively (Supplemental Figure 2). This multilinage differentiation potential was similar to that displayed by bone marrow-derived MSCs (bmMSCs) that were isolated from human bone marrow aspirates to serve as controls. Additionally, watMSCs were serially passaged (up to P10) to determine their expansion potential. We estimated that from 1 g of WAT, $2x10^9$ (accumulated cell number) watMSCs can be obtained in approximately 20 days (P4) and as much as $10^{12}$ watMSCs in 33 days (P7) (Supplemental

Figure 2). This expansion potential was similar to that displayed by bmMSCs isolated from 25 mL of bone marrow aspirates.

To assess the ability of watECFCs to modulate MSC differentiation into SMCs, we cultured them in direct contact with watMSCs that were obtained from the same WAT sample. Cultured MSCs share multiple cellular markers with SMCs (e.g., α-SMA, calponin), therefore, differentiation was assessed by expression of smooth muscle myosin heavy chain (smMHC), a definitive marker of mature SMCs that is not expressed by MSCs. Indeed, in the absence of direct contact with ECFCs, smMHC expression was undetectable in watMSCs (Figure 4A). However, when watMSCs were directly co-cultured with watECFCs for 7 days, expression of smMHC was consistently induced (Figure 4A), indicating smooth muscle myogenic ability. The ability of watECFCs to induce MSC differentiation was quantified and found equal ($P>0.05$) to that displayed by both cbECFCs and pbECFCs (Figure 4B).

**In vivo vasculogenic potential of WAT-derived ECFCs**

To test blood vessel-forming ability, we used our xenograft mouse model [4]; watECFCs were combined with watMSCs and subcutaneously implanted into nude mice for 8 days (Figure 5). Histological examination of explants revealed extensive networks of perfused human microvessels (Figure 5A-C and online Supplemental Figure 3), confirming the lumenal localization of watECFCs. Examination of watECFC-lined vessels showed no histological evidence of thrombosis. Microvessel density in implants that contained watECFCs/watMSCs (67.62 vessels/$mm^2$) was statistically similar to those containing cbECFCs/bmMSCs (145.12 vessels/$mm^2$) and pbECFCs/bmMSCs (80.46 vessels/$mm^2$)($P>0.05$) (Figure 5D). To confirm these histological results, additional implant-bearing mice were injected (i.v.) with rhodamine-conjugated UEA-1 just before removing the implants (online Supplemental Figure 4); cells were then enzymatically retrieved and analyzed by FC. We found that the total number of ECFCs that

engrafted as part of a perfused lumen (hCD31$^{+}$/UEA-1$^{+}$) was statistically similar in implants that contained cbECFCs ($2.3x10^{4}$), pbECFCs ($2.2x10^{4}$), and watECFCs ($2.3x10^{4}$) (Figure 5E) ($P>0.05$). Finally, watECFC-lined microvessels showed equal perivascular coverage than those lined by blood-derived ECFCs, which indicated no differences in their ability to form stable vessels (Figure 5G-I).

**Discussion**

Here, we demonstrated that human WAT is a dependable source of ECFCs with properties similar to those obtained from adult peripheral blood, including a robust ability to form functional blood vessels in vivo. The feasibility of using human ECs to bioengineer a microvascular network that integrates with a host vasculature was first demonstrated with Bcl-2-transduced umbilical vein ECs (HUVECs) [23] and juvenile dermal (foreskin) microvascular ECs (HDMECs) [24]. However, both HUVECs and HDMECs originate from non-adult tissues and thus, they are not readily available for general clinical use. Instead, patients would need to rely on ECs obtained from their aged vascular tissues, but the full vasculogenic potential of mature ECs have not been systematically assessed in the context of tissue engineering. In this regard, the discovery of highly proliferative ECFCs in human peripheral blood created a promising opportunity to non-invasively obtain large quantities of readily available, autologous ECs [1,2]. Over the last few years, we and others have rigorously demonstrated that human adult ECFCs indeed have robust in vivo vasculogenic potential and that when combined with a suitable source of perivascular cells (namely, SMCs or MSCs), ECFCs can generate long-lasting, stable vascular networks in mice that are more extensive and form more rapidly than those shown in earlier reports with other mature ECs [3-7,20]. However, ECFCs are exceedingly rare in adult peripheral blood [2,8,9] and there are increasingly more studies recognizing absence of pbECFCs in a substantial proportion (~30%) of both healthy and non-healthy adult subjects [10-

12]. In addition, the mechanism by which ECFCs are mobilized into circulation remains elusive, and thus the reliability of peripheral blood as a clinical source of ECFCs is a concern.

In response to this uncertainty, we set up this study to test whether ECFCs can be reliably isolated from other alternative human tissue, namely WAT. Previously, Ingram et al. demonstrated that the wall of both the aorta and the umbilical vein contain a complete hierarchy of highly proliferative ECs with equal colony-forming ability to blood-derived ECFCs [16], but whether similar ECFCs are present in human WAT has not been shown to date. To answer this question, we adapted a simple procedure that enables isolating ECs from small (1 g) intact biopsies of normal subcutaneous WAT (no liposuction aspirates were used) by enzymatic digestion followed by selection of $CD31^+$ cells. Subsequently, we extensively interrogated the entire WAT-derived EC population, compared it to bonafide blood-derived ECFCs, and unequivocally demonstrated that the vasculature of human WAT is indeed a dependable source of ECFCs. We showed that WAT has a hierarchical distribution of watECFCs with colony-forming ability that was consistent with that of adult blood-derived ECFCs [2]. The percentage of ECFCs with colony-forming potential (>3 divisions) was 7% and 15% for watECFCs and pbECFCs, respectively.

Our study has revealed several characteristics that make WAT an advantageous alternative for the obtention of ECFCs. First, unlike adult peripheral blood, WAT was found to be a very reliable source of ECFCs, with 100% (5/5) success rate observed in this study. Second, watECFC cultures were highly pure (>96%) and the presence of other stromal contaminants (namely, hematopoietic or mesenchymal cells) was negligible. Third, watECFCs had remarkable expansion potential. We showed that $10^9$ homogeneous watECFCs can be obtained from 1 g of WAT after 30 days in culture; this cell number is likely to be sufficient considering what would be needed for most cell-based applications. Also, WAT biopsies exceeding 1 g can easily be

harvested without increasing morbidity, which would proportionally amplify cell yield. To put this into perspective, the replicative capacity we have shown for watECFCs is lower than that reported for neonatal cbECFCs but similar to adult pbECFCs [2,3,15]. Fourth, similarly to blood-derived ECFCs, watECFCs had a stable phenotype. We demonstrated that culture expanded watECFCs robustly displayed endothelial properties and functions, as confirmed by (i) the expression of EC markers (CD31, VE-cadherin, vWF, eNOS, VEGFR-2); (ii) uptake of Ac-LDL; (iii) binding of UEA-1 lectin; (iv) capillary-like network formation ability; (v) response to angiogenic growth factors (VEGF, bFGF); and (vi) up-regulation of adhesion molecules (E-selectin, ICAM-1) upon exposure to TNF-α and subsequent increase in leukocyte binding. Fifth, culture expanded watECFCs had a robust in vivo vasculogenic potential. Without exception, in all WAT-derived ECFCs tested, co-implantation with watMSCs into immunodeficient mice rapidly generated an extensive network of human blood vessels with watECFCs specifically lining the lumens and MSCs occupying perivascular position. Importantly, we found no differences between pbECFCs and watECFCs in terms of ability to form microvessels with extensive perivascular coverage, as accounted by both FC and histology. Collectively, our study has revealed not only that watECFCs were undoubtedly ECs, but also that WAT- and blood-derived ECFCs were phenotypically highly similar.

Finally, an important additional advantage of WAT is the well-recognized presence of MSCs (watMSCs) [6,25], which eliminates the need for bone marrow biopsies in our effort to bioengineer microvascular networks. Indeed, we isolated watMSCs from the $CD31^-$ cell fraction of WAT and demonstrated their similarities with bone marrow-derived MSCs, including (i) expansion potential, (ii) multi-lineage differentiation potential, and (iii) ability to modulate ECFC function both in vitro and in vivo. Of note, watMSCs were susceptible to undergoing smooth muscle myogenic differentiation in the presence of all three types of ECFCs (watECFCs,

cbECFCs, and pbECFCs), with no significance difference among any of them. This myogenic susceptibility was identical to that of bmMSCs, as previously reported [4].

In conclusion, we found that human WAT is a reliable source of ECFCs with properties similar to those obtained from adult peripheral blood, including a robust ability to form functional blood vessels in vivo. For well over a decade, the possibility of obtaining autologous ECFCs from a simple blood draw created widespread excitement. However, considering (1) the unreliability and low rate of occurrence of ECFCs in adult peripheral blood, (2) our limited understanding of how pbECFCs are mobilized into circulation, and (3) the fact that biopsies of WAT can be obtained with minimal intervention in an ambulatory setting, we foresee WAT as a more practical alternative to obtain large amounts of readily available autologous ECFCs. Further studies assessing the clinical potential of watECFCs in aging adults and in health and disease are warranted.

**Acknowledgments**

We thank Drs. Kyu-Tae Kang and Joyce Bischoff (Vascular Biology Program, Boston Children's Hospital) for kindly providing some pbECFCs. This work was supported by a National Institutes of Health grant (R00EB009096, J.M.-M).

**Conflict of Interest**

The authors have declared that no conflict of interest exists.

**References**


1. Lin Y, Weisdorf DJ, Solovey A, Hebbel RP (2000) Origins of circulating endothelial cells and endothelial outgrowth from blood. J Clin Invest 105(1), 71–77

2. Ingram DA, Mead LE, Tanaka H, et al (2004) Identification of a novel hierarchy of endothelial progenitor cells using human peripheral and umbilical cord blood. Blood 104(9), 2752–2760

3. Melero-Martin J, Khan ZA, Picard A, Wu X, Paruchuri S, Bischoff J (2007) In vivo vasculogenic potential of human blood-derived endothelial progenitor cells. Blood 109(11), 4761–4768

4. Melero-Martin J, De Obaldia ME, Kang S-Y, et al (2008) Engineering robust and functional vascular networks in vivo with human adult and cord blood-derived progenitor cells. Circ Res 103(2), 194–202

5. Au P, Daheron LM, Duda DG, et al (2007) Differential in vivo potential of endothelial progenitor cells from human umbilical cord blood and adult peripheral blood to form functional long-lasting vessels. Blood 111(3), 1302–1305

6. Traktuev DO, Prater DN, Merfeld-Clauss S, et al (2009) Robust functional vascular network formation in vivo by cooperation of adipose progenitor and endothelial cells. Circ Res 104(12), 1410–1420

7. Chen X, Aledia AS, Popson SA, Him L, Hughes CCW, George SC (2010) Rapid anastomosis of endothelial progenitor cell-derived vessels with host vasculature is promoted by a high density of cotransplanted fibroblasts. Tissue Eng Part A 16(2), 585–594

8. Gulati R, Jevremovic D, Peterson TE, et al (2003) Diverse origin and function of cells with endothelial phenotype obtained from adult human blood. Circ Res 93(11), 1023–1025

9. Yoder MC, Mead LE, Prater D, et al (2007) Redefining endothelial progenitor cells via clonal analysis and hematopoietic stem/progenitor cell principals. Blood 109(5), 1801–1809

10. Rignault-Clerc S, Bielmann C, Delodder F, et al (2012) Functional late outgrowth endothelial progenitors isolated from peripheral blood of burned patients. Burns doi:pii: S0305-4179(12)00320-8. 10.1016/j.burns.2012.09.027. [Epub ahead of print]

11. Stroncek JD, Grant BS, Brown MA, Povsic TJ, Truskey GA, Reichert WM (2009) Comparison of endothelial cell phenotypic markers of late-outgrowth endothelial progenitor cells isolated from patients with coronary artery disease and healthy volunteers. Tissue Eng Part A 15(11), 3473–3486

12. Thill M, Strunnikova NV, Berna MJ, et al (2008) Late outgrowth endothelial progenitor cells in patients with age-related macular degeneration. Invest Ophthalmol Vis Sci 49(6), 2696–2708

13. Bompais H, Chagraoui J, Canron X, et al (2004) Human endothelial cells derived from circulating progenitors display specific functional properties compared with mature vessel wall endothelial cells. Blood 103(7), 2577–2584

14. Yang J, Chang E, Cherry AM, et al (1999) Human endothelial cell life extension by telomerase expression. J Biol Chem 274(37), 26141–26148

15. Hur J, Yoon C-H, Kim H-S, et al (2004) Characterization of two types of endothelial progenitor cells and their different contributions to neovasculogenesis. Arterioscler Thromb Vasc Biol 24(2), 288–293

16. Ingram DA, Mead LE, Moore DB, Woodard W, Fenoglio A, Yoder MC (2005) Vessel wall-derived endothelial cells rapidly proliferate because they contain a complete hierarchy of endothelial progenitor cells. Blood 105(7), 2783–2786

17. Yoder MC. Is endothelium the origin of endothelial progenitor cells? (2010) Arterioscler Thromb Vasc Biol 30(6), 1094–1103

18. Kern PA, Knedler A, Eckel RH (1983) Isolation and culture of microvascular endothelium from human adipose tissue. J Clin Invest 71(6), 1822–1829

19. Szöke K, Beckstrøm KJ, Brinchmann JE (2012) Human adipose tissue as a source of cells with angiogenic potential. Cell Transplant 21(1), 235–250

20. Lin R-Z, Moreno-Luna R, Zhou B, Pu WT, Melero-Martin J (2012) Equal modulation of endothelial cell function by four distinct tissue-specific mesenchymal stem cells. Angiogenesis 15(3), 443–455

21. Lin R-Z, Dreyzin A, Aamodt K, et al (2011) Induction of erythropoiesis using human vascular networks genetically engineered for controlled erythropoietin release. Blood 118(20), 5420–5428

22. Pittenger MF, Mackay AM, Beck SC, et al (1999) Multilineage potential of adult human mesenchymal stem cells. Science 284(5411), 143–147

23. Schechner JS, Nath AK, Zheng L, et al (2000) In vivo formation of complex microvessels lined by human endothelial cells in an immunodeficient mouse. Proc Natl Acad Sci USA 97(16), 9191–9196

24. Nör JE, Peters MC, Christensen JB, et al (2001) Engineering and characterization of functional human microvessels in immunodeficient mice. Lab Invest 81(4), 453–463

25. Crisan M, Yap S, Casteilla L, et al (2008) A perivascular origin for mesenchymal stem cells in multiple human organs. Cell Stem Cell. 3(3), 301–313

**Figures captions**

**Figure 1. Isolation and culture expansion of ECFCs from human WAT.** (A) Human watECFCs were isolated from subcutaneous WAT after enzymatic digestion and were purified from the stromal vascular fraction (SVF) using CD31-coated magnetic beads. (B-C) Phase contrast micrographs of (B) a colony (scale bar: 500 μm) and (C) a confluent monolayer of watECFCs with characteristic cobble-stone morphology (scale bar: 200 μm). (D) Expansion potential of watECFCs measured by accumulative cell number in serially passaged cells. (E-G) Cloning-forming ability of watECFCs was examined at clonal density and compared to cord and peripheral blood-derived ECFCs (passage 2). (E) The endothelial nature of the colonies was confirmed by binding of UEA-1 lectin (scale bar: 500 μm). (F) Percentage of cells with cloning ability (>8 cells) after 10 days. (G) Colonies were categorized into large (>300 cells), medium (100-300 cells) and small (8-100 cells) size. All bars represent mean ± S.D. from three independent samples. * $P<0.05$ between watECFCs and pbECFCs. † $P<0.05$ between watECFCs and cbECFCs. (n.s.) $P>0.05$ between watECFCs and both pbECFCs and cbECFCs.

**Figure 2. Phenotypical characterization of watECFCs.** (A) Indirect immunofluorescence of watECFCs showed positive staining for CD31, vWF, and VE-cadherin. IgG control depicted in inset. Cell nuclei were counterstained with DAPI (scale bar: 100 μm). (B) Flow cytometry analysis of watECFCs for CD31, CD90, and CD45. Black line histograms represent cells stained with fluorescent antibodies. Isotype-matched controls are overlaid in solid gray histograms. (C) Quantitative RT-PCR analyses of ECFCs for endothelial (CD31, vWF, VE-Cadherin, VEGFR2, eNOS) and mesenchymal (CD90, PDGFRβ) markers. (D) Binding of UEA-1 lectin to watECFCs. IB4 lectin served as negative control (inset) (scale bar: 50 μm). (E) watECFCs uptake of fluorescently labeled Ac-LDL (Dil-Ac-LDL) (scale bar: 50 μm). MSCs served as negative uptake control (inset).

**Figure 3. In vitro functional characterization of watECFCs.** (A) Proliferation of ECFCs after 48 h in response to VEFG-A (10 ng/mL) and FGF-2 (1 ng/mL). Cell number were normalized to those obtained with basal medium. (B) Migration in response to VEGF-A (10 ng/mL) and FGF-2 (1 ng/mL). Representative micrographs of scratched watECFCs after 24 h in basal and FGF-2-containing medium (dashed line delineate the scratch; scale bar: 500 μm). Scratch size was quantified at 24 h as percentage of original size. (C) Representative micrograph of watECFC-lined capillary-like network on a Matrigel-coated plate (scale bar: 500 μm). Total tube length quantified at 24 h. (D) Up-regulation of E-selectin and ICAM-1 in response to TNF-α. Representative flow cytometry histograms depicted for watECFCs. Red line histograms represent cells stimulated with TNF-α, while solid gray histograms represent untreated controls. (E) Representative micrographs of watECFC with an increased number of bound HL-60 leukocytes after TNF-α treatment compared to untreated control (scale bar: 200 μm). Quantification of bound leukocytes per unit of area for each of ECFC group. All bars represent mean ± S.D. from three independent samples. * $P<0.05$ between watECFCs and pbECFCs. † $P<0.05$ between watECFCs and cbECFCs. (n.s.) $P>0.05$ between watECFCs and both pbECFCs and cbECFCs.

**Figure 4. Smooth muscle cell differentiation of watMSCs.** Smooth muscle myogenic differentiation was evaluated by culturing watMSCs in the presence of ECFCs for 7 days. Induction of SMC phenotype was assessed by the expression of smMHC (smMHC-FITC). Expression of vWF (vWF-Texas Red) was used to detect ECFCs and DAPI for cell nuclei. (A) Representative immunofluorescent images of watMSCs in the absence or presence of various types of ECFCs. smMHC was absent in monocultures of watMSCs (left panel), but it was induced when co-cultured with watECFCs, cbECFCs, and pbECFCs (scale bar: 100 μm). (B) Quantification of smooth muscle myogenic differentiation as number of MSCs expressing

smMHC per unit of culture area. All bars represent mean ± S.D. from three independent samples. (n.s.) P>0.05 between watMSCs and bmMSCs and between all three types of ECFCs.

**Figure 5. In vivo vasculogenic potential of watECFCs.** ECFCs were combined with MSCs in collagen-fibrin gel and the mixture subcutaneously injected into nude mice for 8 days. (A) H&E from one representative watECFC explant (inset, scale bar: 5 mm) with numerous blood vessels (yellow arrowheads; scale bar: 50 μm). (B-C) Immunohistochemistry (hCD31) showed human specific lumens (yellow arrowheads; scale bars: 50 μm). (D) Microvessel density determined as luminal structures containing erythrocytes. (E) Rhodamine-conjugated UEA-1 was injected (i.v.). 10 min before implants were excised. The number of ECFCs that were part of a perfused lumen ($hCD31^+/UEA\text{-}1^+$) was quantified by FACS. (F) hCD31 (green) immunofluorescent staining of a representative UEA-1+ (red) microvessel in a watECFC explant (scale bar: 20 μm). (G-H) Perivascular coverage was assessed by double immunofluorescent staining of explants with UEA-1 (red) and α-smooth muscle actin (α- SMA; green). Images are representative of all watECFC explants. Nuclei were counterstained with DAPI (scale bars: 50 μm). (I) Percentage of human $UEA\text{-}1^+$ blood vessels covered by $\alpha\text{-}SMA^+$ perivascular cells. Human dermis served as control. All bars represent mean ± S.D. from three independent samples. * P<0.05 between watECFCs and pbECFCs. † P<0.05 between watECFCs and cbECFCs. (n.s.) P>0.05 between watECFCs and both pbECFCs and cbECFCs.

Figure 1
Click here to download high resolution image

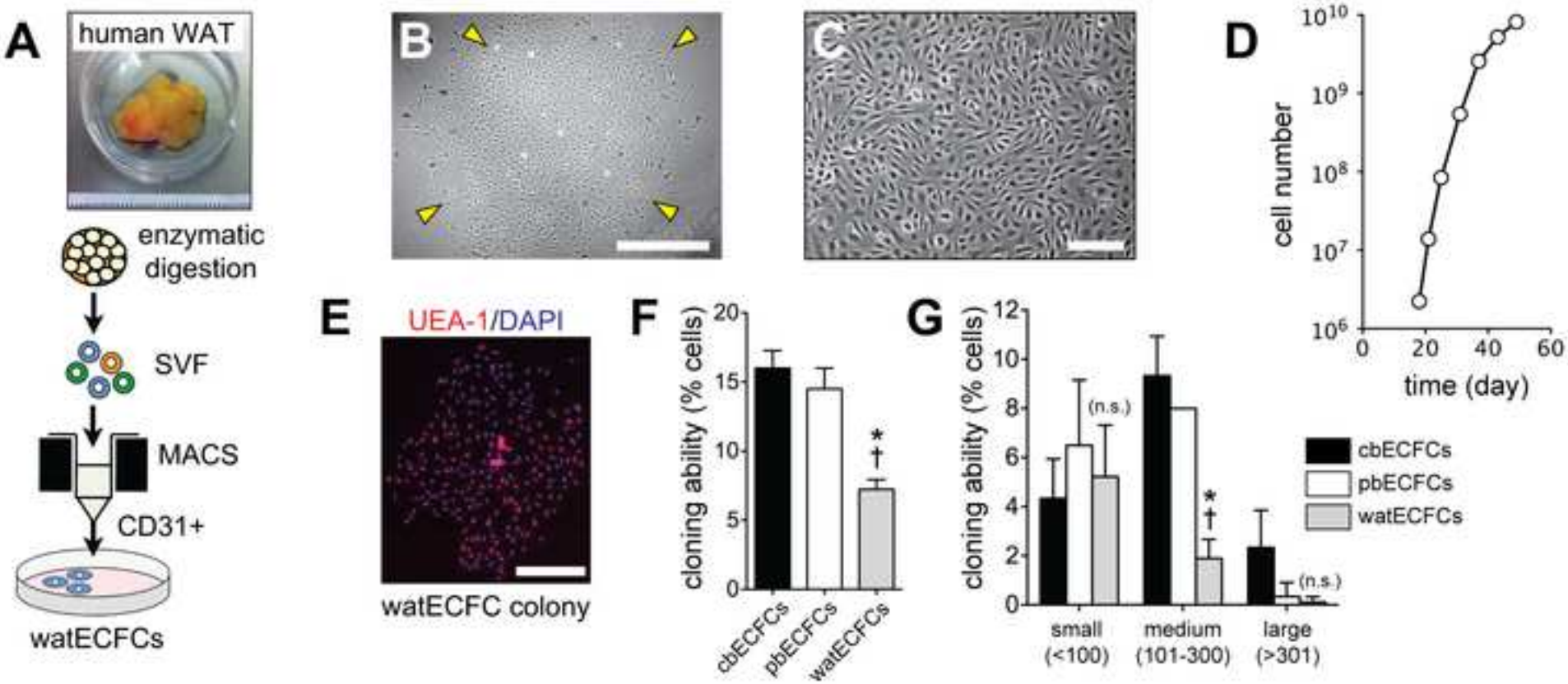

Figure 2
Click here to download high resolution image

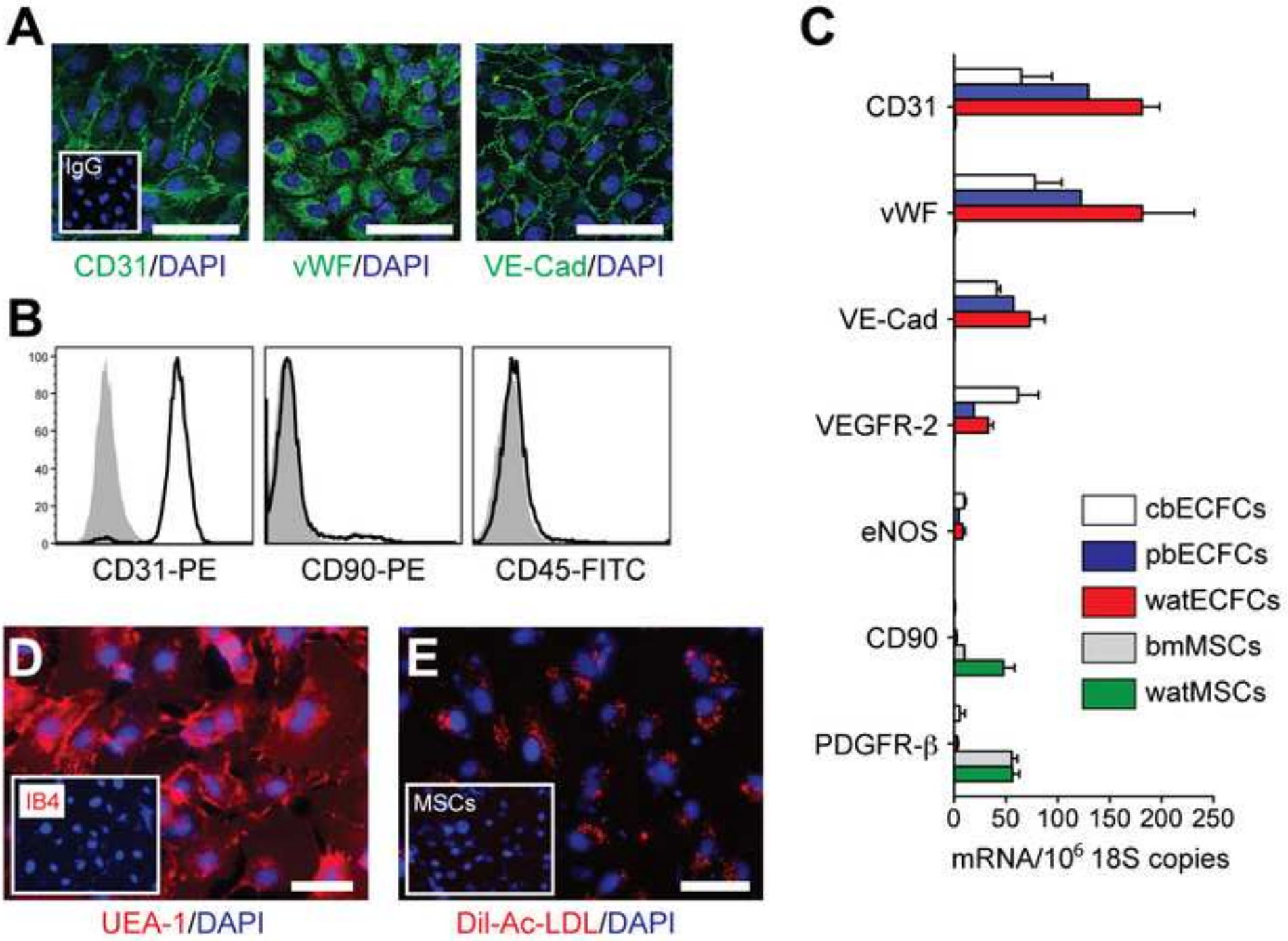

Figure 3
Click here to download high resolution image

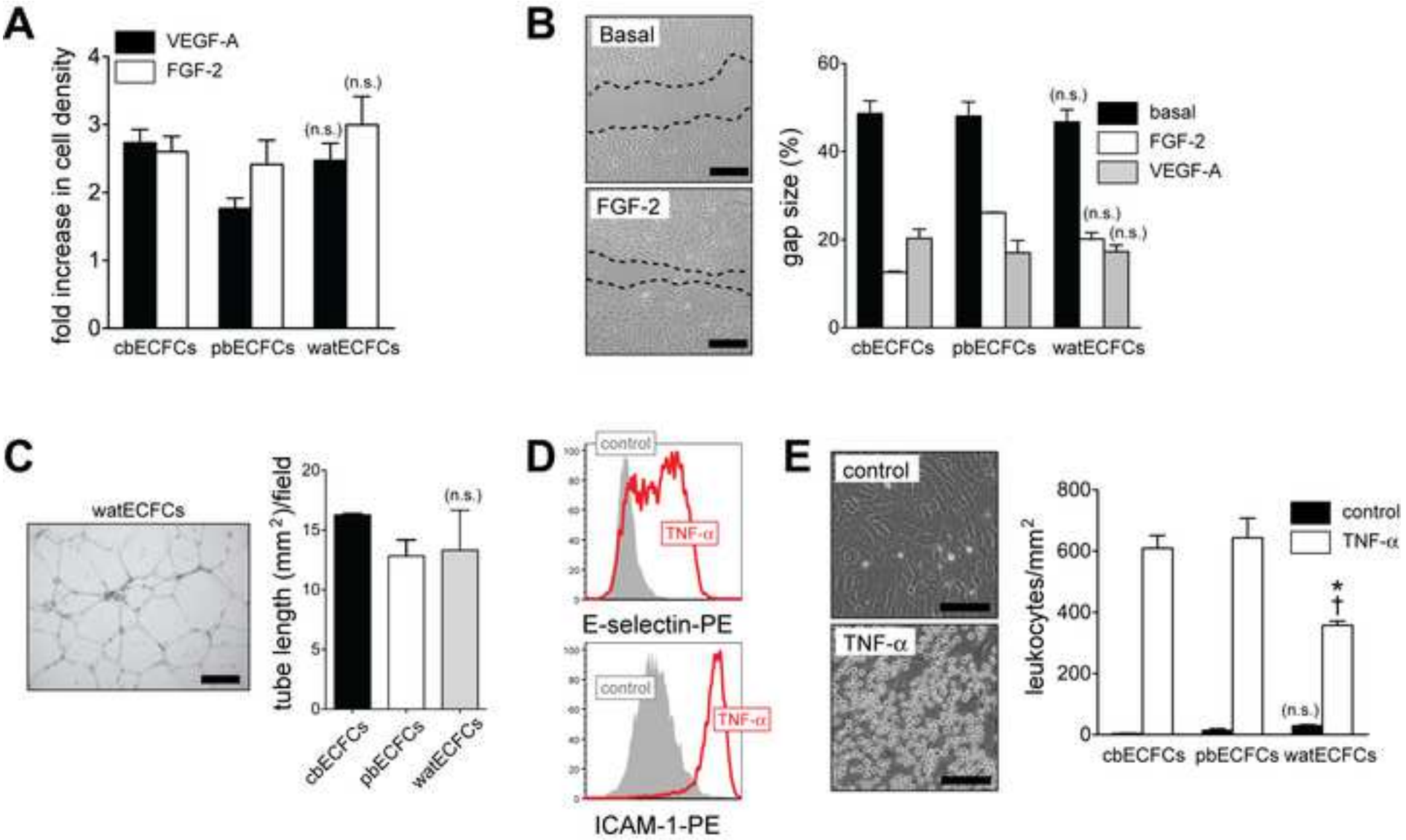

Figure 4
Click here to download high resolution image

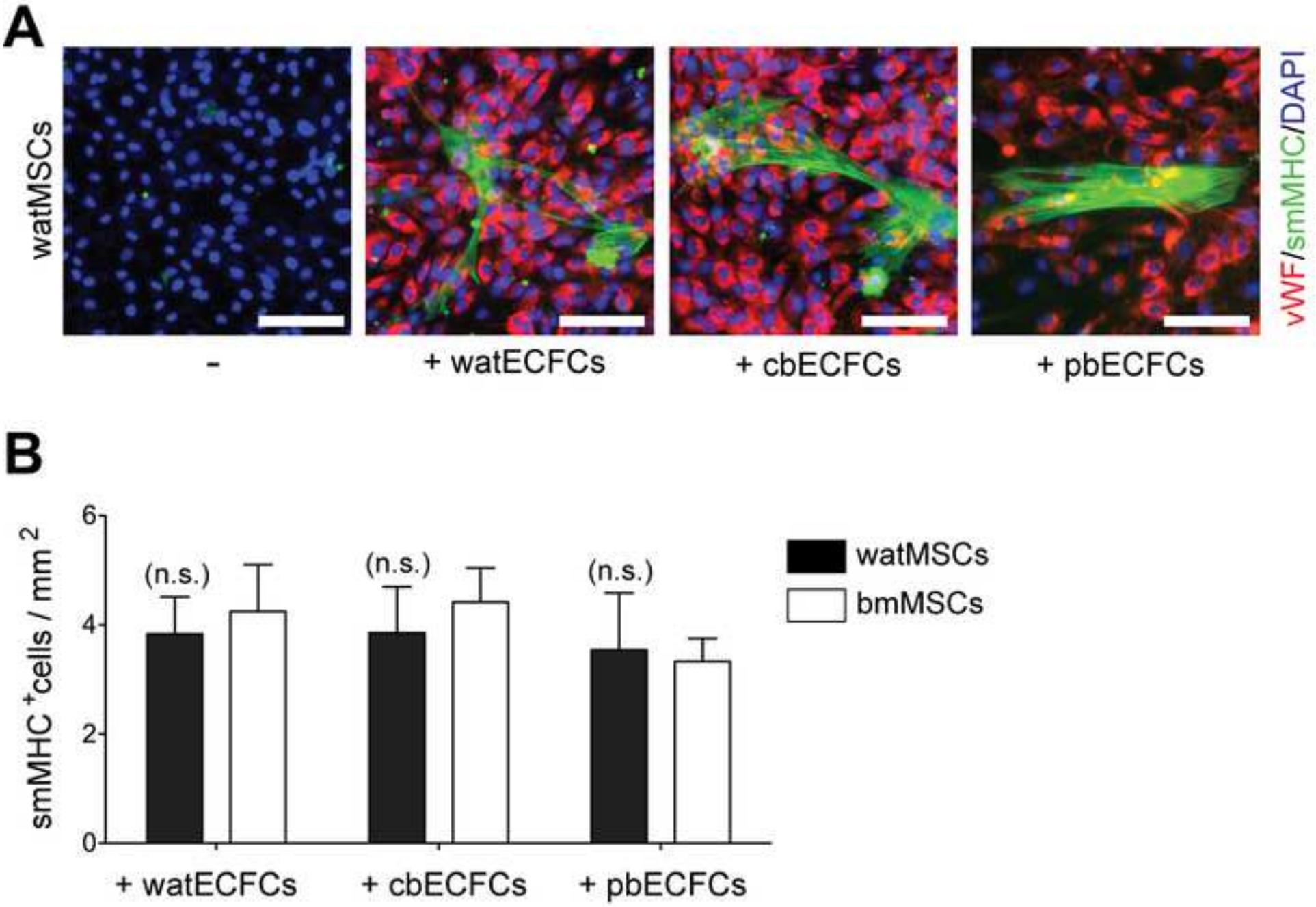

Figure 5
Click here to download high resolution image

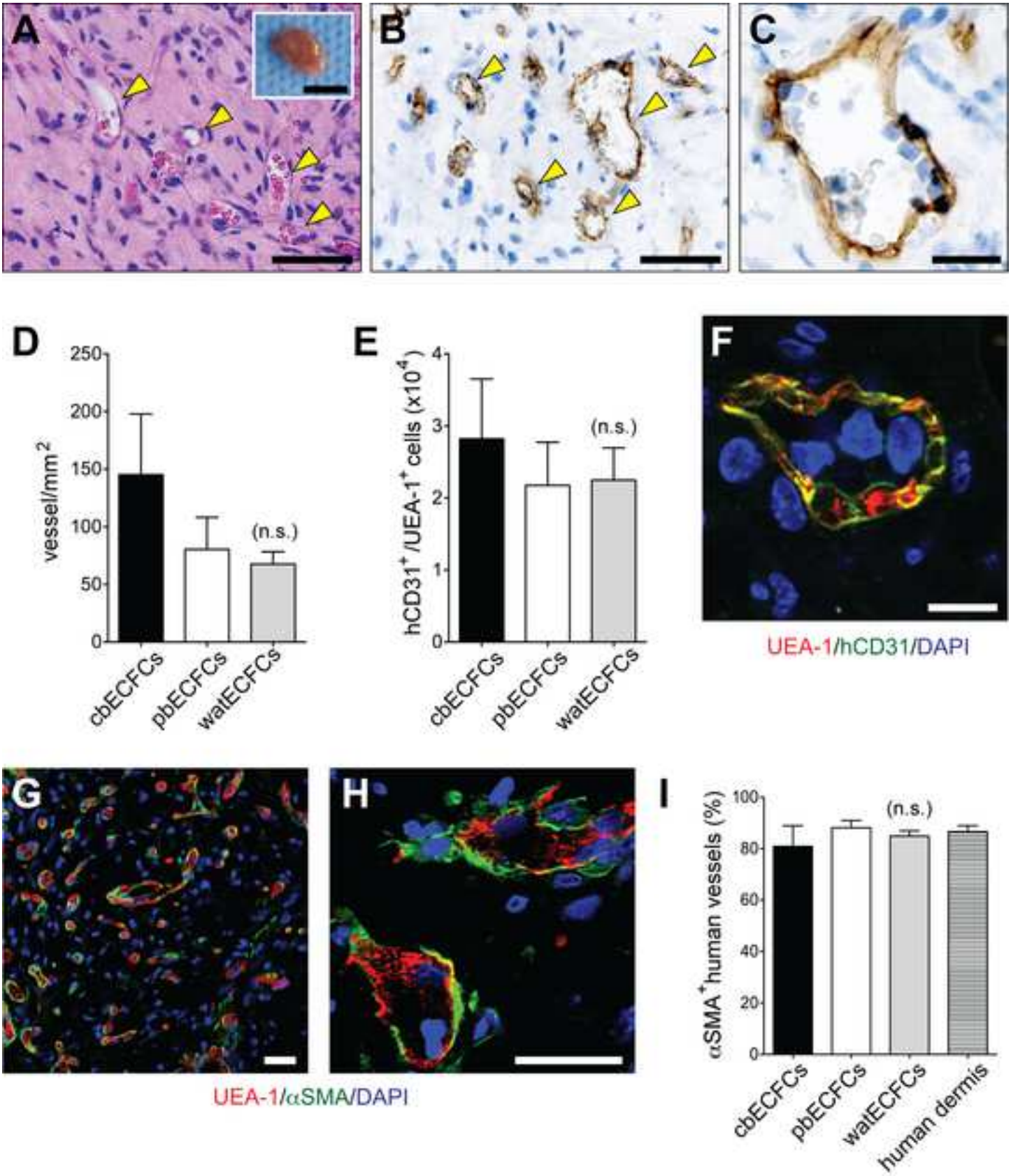

## SUPPLEMENTAL MATERIAL

## DETAILED METHODS

### Isolation of ECFCs and MSCs from white adipose tissue (WAT)

Normal discarded subcutaneous WAT samples (n=5) were obtained during a clinically-indicated procedure in accordance with an Institutional Review Board-approved protocol. WAT samples were washed, minced and enzymatically (collagenase and dispase) digested for 1h at 37°C. The stromal vascular fraction (SVF) was obtained after removal of mature adipocytes by centrifugation (450xg for 10 min) and the lysis of erythrocytes with ammonium chloride solution [1]. watECFCs were purified by magnetic activated cell sorting (MACS) using CD31-coated magnetic beads (Dynalbeads; Invitrogen, Grand Island, NY). CD31-selected watECFCs were cultured on 1% gelatin-coated plates using ECFC-medium: EGM-2 (except for hydrocortisone; Lonza, Walkersville, MD) supplemented with 20% FBS (Atlanta Biological, Lawrenceville, GA), 1x glutamine-penicillin-streptomycin (GPS; Invitrogen, Carlsbad, CA). watMSCs were obtained from the $CD31^-$ cell fraction of the SVF and were cultured onto non-coated plates using MSC-medium: MSCGM Mesenchymal Stem Cell Medium BulletKit (basal media and SingleQuots; Lonza), supplemented with 10 % FBS (MSC-Qualified; Invitrogen), 1xGPS (Invitrogen), and 10 ng/mL of FGF-2 (R&D Systems, Minneapolis, MN).

### Isolation of ECFCs from blood

Human blood samples were obtained in accordance with Institutional Review Board-approved protocols. Blood-derived ECFCs were obtained as previously described [2,3]. Briefly, ECFCs were isolated from the mononuclear cell (MNC) fractions, after Ficoll-Paque (GE Healthcare, Pittsburgh, PA) density gradient centrifugation, of both cord blood (cbECFCs) and adult peripheral blood (pbECFCs) samples, and purified using CD31-coated magnetic beads. ECFCs were cultured on 1% gelatin-coated plates using ECFC-medium.

**Isolation of MSCs from bone marrow**

Human bmMSCs were isolated from the MNC fraction of 25 mL bone marrow aspirates samples (Lonza) after Ficoll-Paque density gradient centrifugation, as previously described [3]. MNCs were seeded on non-coated tissue culture plates using MSC-medium. Unbound cells were removed at 48 hours, and the bound cell fraction maintained in culture until 70% confluence using MSC-medium.

**Expansion potential**

watECFCs were expanded for 50 days. All passages were performed by plating the cells onto 1% gelatin-coated tissue culture plates at $5x10^3$ cell/$cm^2$ using ECFC-medium. watMSCs and bmMSCs were expanded for 50 days, and all the passages were performed by plating the cells onto non-coated tissue culture plates at $10^4$ cell/$cm^2$ using MSC-medium. Medium was refreshed every 2 to 3 days and cells were harvested by trypsinization and replated in the same culture conditions for the next passage. Cumulative values of total cell number were calculated by counting the cells at the end of each passage using a hemocytometer.

**Colony-forming assay**

Passage 2 (P2) ECFCs were culture for 10 days at clonal density (200 cell/60 $cm^2$; 600 cells plated; n=3 per ECFC type) onto 1% gelatin-coated plates using ECFC-medium. Medium was refreshed every 4 days. At day 10, colonies containing 8 or more cells (i.e., at least 3 divisions) were scored under a fluorescence microscope after DAPI staining of the nuclei. Endothelial phenotype was confirmed by binding of rhodamine-labeled *Ulex Europaeus Agglutinin I* (UEA-1; 1:100; Vector Laboratories, Burlingame, CA) using a fluorescent microscope. Colonies were categorized into large (>300 cells), medium (100-300 cells) and small (8-100 cells) size. The number of cells in each colony was quantified under a fluorescent microscope after DAPI staining using ImageJ analysis software (NIH, Bethesda, MD, USA).

**Flow cytometry**

Cytometric analyses were carried out by labeling with phycoerythrin (PE)-conjugated mouse anti-human CD31 (Ancell, Bayport, MN), PE-conjugated mouse anti-human CD90 (BD Biosciences, San Jose, CA), fluorescein isothiocyanate (FITC)-conjugated mouse anti-human CD45 (BD Biosciences), FITC-mouse IgG1 (BD Biosciences), and PE-mouse IgG1 (BD Biosciences) antibodies (1:100). Antibody labeling was carried out for 20 min on ice followed by 3 washes with 1% BSA, 0.2 mM EDTA in PBS and resuspension in 1% paraformaldehyde in PBS. Flow cytometric analyses were performed using a Guava easyCyte 6HT/2L flow cytometer (Millipore Corporation, Billerica, MA) and FlowJo software (Tree Star Inc., Ashland, OR). Human mesenchymal stem cells (MSCs) served as controls.

**Indirect immunofluorescence**

Immunofluorescence was carried out using mouse anti-human CD31 (1:200; DakoCytomation, Carpinteria, CA), mouse anti-human vWF (1:200; DakoCytomation), and goat anti-human VE-cadherin (1:200; Santa Cruz Biotechnology, Santa Cruz, CA) antibodies, followed by FITC-conjugated secondary antibodies (1:200; Vector Laboratories) and Vectashield mounting medium with DAPI (Vector Laboratories). Human MSCs served as controls.

**RT-PCR and multigene transcriptional profiling**

Total RNA was isolated with a RNeasy kit (QIAGEN, Valencia, CA), and cDNA was prepared using reverse transcriptase III (Invitrogen). Multigene transcriptional profiling was used to determine the number of mRNA copies per cell normalized to 18S rRNA abundance (~$10^6$ 18S-rRNA copies/cell) [4]. Real-time PCR primer sequences were as follows: human CD90 (hCD90; Thy1) (F:GCCTAACGGCCTGCCTAGT, R:GGGTGAACTGCTGGTATTCTCAT); human CD31 (hCD31; PECAM1) (F:CACCTGGCCCAGGAGTTTC, R:AGTACACAGCCTTGTTGCCATGT); human vWF (hvWF) (F:GTCGAGCTGCACAGTGACATG, R:GCACCATAAACGTTGACTTCCA); human VE-Cadherin (VE-Cad.; CD144) (F:GAACCCAAGATGTGGCCTTTAG, R: ATGTGACAA-

CAGCGAGGTGTAA); human VEGFR2 (F:GGCAAATGTGTCAGCTTTGTACA, R: GTCACGTG-GAAGGAGATCAC); human eNOS (NOS3) (F:AGATCTCCGCCTCGCTCAT, R:GTCTCGGAGC-CATACAGGATTG); human PDGFRβ (CD140b)(F:GGTGGGCACACTACAATTTGC, R:GGTG-GGTAGGCCTCGAACA).

**Binding of *Ulex Europaeus Agglutinin* lectin**

Confluent monolayers of ECFCs were incubated with rhodamine-labeled UEA-1 (Vector Laboratories; final concentration: 20 µg/mL) in ECFC-medium for 30 min. Cells were washed three times in ECFC-medium, fixed in 4% paraformaldehyde in PBS and cell nuclei stained with DAPI. Cells were visualized under a fluorescent microscope.

**Uptake of Ac-LDL**

Confluent monolayers of ECFCs were incubated with DiI-Ac-LDL (Invitrogen; final concentration: 5 µg/mL) in ECFC-medium for 8 h. Cells were washed three times in ECFC-medium, fixed in 4% paraformaldehyde in PBS and cell nuclei stained with DAPI. Cells were visualized under a fluorescent microscope.

**Proliferation assay**

ECFCs were seeded in triplicate onto fibonectin-coated 24-well plates at $5x10^3$ cell/$cm^2$ using basal medium (EBM-2, 5% FBS). Plating efficiency was determined at 24 h. Cells were then treated for 48 h using basal medium in the presence or absence of either 10 ng/mL VEGF-A or 1 ng/mL FGF-2 (R&D Systems). Cells were quantified under a fluorescent microscope after DAPI staining using ImageJ analysis software; results were normalized to cell number obtained in basal medium.

**Scratch assay**

The scratch assay was performed in confluent cultures of ECFCs plated on 6-well plates. Scratch wounds were generated across each well using a pipette tip. Cells were then treated for 24 h using basal medium in the presence or absence of 10 ng/mL VEGF-A or 1 ng/mL FGF-2. Scratch size was measured after 24 h under a phase contrast microscope.

**Tube formation assay**

ECFCs were seeded on Matrigel-coated plates at a density of $2x10^4$ cell/$cm^2$ and incubated for 24 h in ECFC-medium. The total length of ECFC-lined cords were measured using ImageJ analysis software.

**Up-regulation of leukocyte adhesion molecules**

ECFC monolayers were challenged with or without 10 ng/ml of tumor necrosis factor-α (TNF-α; R&D Systems) for 5 h. Afterwards, the leukemia cell line HL-60 ($2x10^6$ cells) was added and incubated at 4°C on a rocking platform for 45 min. Bound leukocytes were visualized using a phase contrast microscope and quantified with ImageJ analysis software. Additionally, leukocyte adhesion molecules were analyzed by flow cytometry using PE-conjugated antibodies against human E-selectin and ICAM-1 (1:100; BD Biosciences).

**Adipogenic differentiation of MSCs**

Confluent MSCs were cultured for 10 days in low-glucose DMEM with 10 % FBS, 1x GPS, and adipogenic supplements (5 µg/mL insulin, 1 µM dexamethasone, 0.5 mM isobutylmethylxanthine, 60 µM indomethacin, 1 µM rosiglitazone). Differentiation into adipocytes was assessed by Oil Red O staining. Cells cultured in medium lacking adipogenic supplements served as a negative control.

**Osteogenic differentiation of MSCs**

Confluent MSCs were cultured for 21 days in low-glucose DMEM with 10 % FBS, 1x GPS, and osteogenic supplements (1 μM dexamethasone, 10 mM β-glycerophosphate, 60 μM ascorbic acid-2-phosphate). Differentiation into osteocytes was assessed by Alizarin Red and von Kossa staining. Cells cultured in medium lacking osteogenic supplements served as a negative control.

**Chondrogenic differentiation of MSCs**

Suspensions of MSCs were gently centrifuged in 15 mL polypropylene centrifuge tubes (500,000 cells/tube). The pellets were cultured in high-glucose DMEM medium with 1x GPS, and chondrogenic supplements (1x insulin–transferrin–selenium, 1 μM dexamethasone, 100 μM ascorbic acid-2-phosphate, and 10 ng/mL TGF-β3). After 21 days, pellets were fixed in 10 % buffered formalin, cryoprotected in 30 % (w/v) sucrose solution, embedded in O.C.T. medium, and sectioned (8 μm-thick) using a cryostat microtome. Differentiation into chondrocytes was assessed by evaluating the presence of glycosaminoglycans after Alcian Blue staining. Cells cultured in the absence of TGF-β3 served as negative controls and failed to form compact spheroids.

**Smooth muscle myogenic differentiation of MSCs**

MSCs were co-cultured for 7 days with ECFCs (1:1 ratio) on fibonectin-coated, 2-well Permanox chamber slides at a density of $10^5$ cell/well using ECFC-medium. MSC expression of smooth muscle myosin heavy chain (smMHC) was evaluated by immunofluorescence using a rabbit monoclonal antibody (1:200; Biomedical Technologies, Stoughton, MA) followed by anti-rabbit FITC-conjugated secondary antibody (1:200; Vector Laboratories). ECFCs were stained with mouse anti-human vWF (1:200; DakoCytomation) followed by Texas Red-conjugated secondary antibody (1:200; Vector Laboratories). Monocultures of MSCs cultured in ECFC-medium served as negative control. Quantification was carried out in numerous regions from replicated cultures by enumerating the number of smMHC-expressing MSCs per unit of area.

**in vivo vasculogenic assay**

Six-week-old athymic nu/nu mice were purchased from Massachusetts General Hospital (Boston, MA). Mice were housed in compliance with Boston Children's Hospital guidelines, and all animal-related protocols were approved by the Institutional Animal Care and Use Committee. Vasculogenesis was evaluated in vivo using our xenograft model as previously described [5]. Briefly, ECFCs and MSCs ($2x10^6$ total; 2:3 ECFC/MSC ratio) were resuspended in 200 µl of collagen/fibrin–based solution (3 mg/mL of bovine collagen, 30 ug/mL of human fibronectin, 25mM HEPES, 10% 10x DMEM, 10% FBS, and 3 mg/mL of fibrinogen, pH neutral). Before cell injection, 50 uL of 10 U/mL thrombin was subcutaneously injected. All experiments were carried out in 4 mice.

**Histology and immunohistochemistry**

Implants were removed from euthanized mice, fixed in 10% buffered formalin overnight, embedded in paraffin, and sectioned (7-µm-thick). Hematoxylin and eosin (H&E) stained sections were examined for the presence of blood vessels containing red blood cells. For immunohistochemistry, sections were deparaffinized, and antigen retrieval was carried out by heating the sections in Tris-EDTA buffer (10 mM Tris-Base, 2 mM EDTA, 0.05% Tween-20, pH 9.0). The sections were blocked for 30 min in 5-10% blocking serum and incubated with primary antibodies for 1h at RT. The following primary antibodies were used: mouse anti-human CD31 (1:50; DakoCytomation, M0823 Clone JC70A), mouse anti-human α-SMA (1:200; Sigma-Aldrich, A2547 Clone 1A4), and mouse IgG (1:50; DakoCytomation). Horseradish peroxidase (HRP)-conjugated mouse secondary antibody (1:200; Vector Laboratories) and 3,3'-diaminobenzidine (DAB) were used for detection of hCD31, followed by hematoxilin counterstaining and Permount mounting. Fluorescent staining were performed using rhodamine-conjugated UEA-1 (20 µg/mL) and FITC-conjugated secondary antibodies (1:200; Vector Laboratories) followed by DAPI counterstaining.

**Microvessel density**

Microvessel density was reported as the average number of erythrocyte-filled vessels (vessels/ $mm^2$) in sections from the middle of the implants as previously described [2]. The entire area of each section was analyzed. Values reported for each experimental condition correspond to mean ± S.D. obtained from four individual mice.

**Quantification of lumenal ECFCs in vivo**

Rhodamine-conjugated UEA-1 (100 uL; 1 mg/mL in normal saline) was intravenously injected into the tail vein of implant-bearing mice 10 min before harvesting the implants at day 8. Implants were removed from euthanized mice, enzymatically (collagenase and dispase) digested for 1 h at 37°C, and the retrieved cells analyzed by FACS after incubation with PerCP-conjugated anti-mouse CD45 (1:100; BD Biosciences), APC-conjugated anti-human CD90 (1:100; BD Biosciences), and FITC-conjugated anti-human CD31 antibodies (1:100; BD Biosciences). ECFCs in each implant were identified as $mCD45^-/hCD31^+$ cells. Perfused ECFCs were identified as $mCD45^-/hCD31^+/UEA\text{-}1^+$ cells.

**Microscopy**

All images were taken with an Axio Observer Z1 inverted microscope (Carl Zeiss, Berlin, Germany) using AxioVision Rel. 4.8 software. Phase microscopy images were taken with an AxioCam MRm camera and 5x/0.16 or 10x/0.3 objective lens. All fluorescent images were taken with an ApoTome.2 Optical sectioning system (Carl Zeiss) and 20x/0.8 or 40x/1.4 oil objective lens. Non-fluorescent images were taken with an AxioCam MRc5 camera using a 40x/1.4 objective oil lens.

**Statistical analysis**

Data were expressed as mean ± S.D. Comparisons between groups were performed by ANOVA followed by Tukey's multiple post-test analysis using Prism Version 4 software (GraphPad). $P<0.05$ was considered statistically significant.

**References**


1. Lin R-Z, Moreno-Luna R, Zhou B, Pu WT, Melero-Martin J (2012) Equal modulation of endothelial cell function by four distinct tissue-specific mesenchymal stem cells. Angiogenesis 15:443–455

2. Melero-Martin J, Khan ZA, Picard A, Wu X, Paruchuri S, Bischoff J (2007) In vivo vasculogenic potential of human blood-derived endothelial progenitor cells. Blood 109:4761–4768

3. Melero-Martin J, De Obaldia ME, Kang S-Y, Khan ZA, Yuan L, Oettgen P, Bischoff J (2008) Engineering robust and functional vascular networks in vivo with human adult and cord blood-derived progenitor cells. Circ Res 103:194–202

4. Shih S-C, Smith LEH (2005) Quantitative multi-gene transcriptional profiling using real-time PCR with a master template. Exp Mol Pathol 79:14–22

5. Lin R-Z, Dreyzin A, Aamodt K, Li D, Jaminet S-CS, Dudley AC, Melero-Martin J (2011) Induction of erythropoiesis using human vascular networks genetically engineered for controlled erythropoietin release. Blood 118:5420–5428

## SUPPLEMENTAL FIGURES

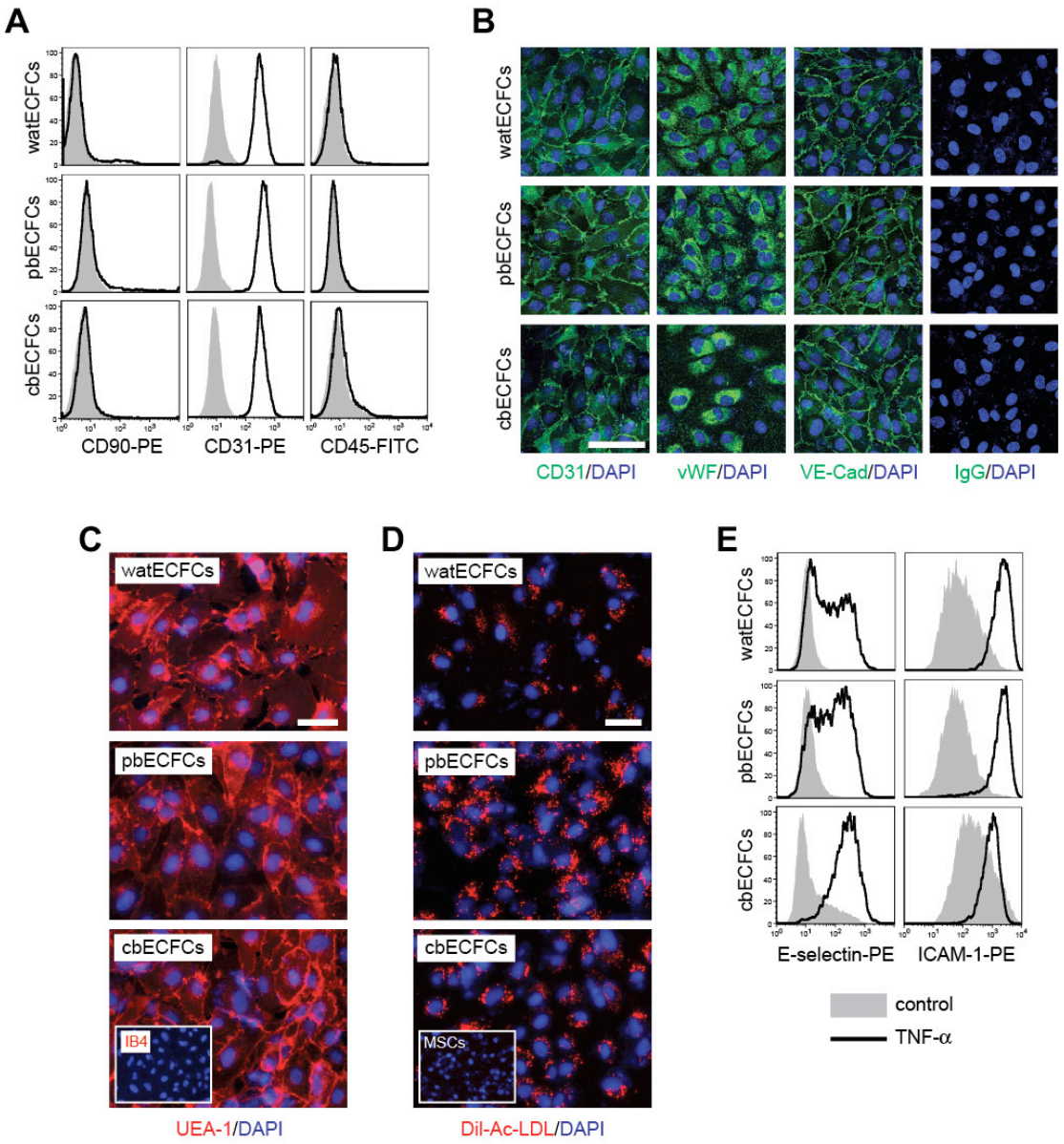


**Supplemental Figure 1. Phenotypical and functional characterization of ECFCs.** (A) Flow cytometry analysis of ECFCs for EC marker CD31, mesenchymal marker CD90, and hematopoietic marker CD45. Black line histograms represent cells stained with fluorescent antibodies. Isotype-matched controls are overlaid in solid gray histograms. (B) Indirect immunofluorescence of ECFCs grown in a confluent monolayer showing positive staining for CD31, vWF, and VE-cadherin. Mouse IgG was used as control. Cell nuclei were counterstained with DAPI (scale bar: 100 μm). (C) Binding of UEA-1 lectin to a monolayer of ECFCs. IB4 lectin served as negative control (inset) (scale bar: 50 μm). (D) ECFCs uptake of fluorescently labeled acetylated-low density lipoproteins (DiI-Ac-LDL) (scale bar: 50 μm). MSCs served as negative uptake control (inset). (E) Up-regulation of E-selectin and ICAM-1 in cultured ECFCs in response to TNF-α. Black line histograms represent cells stimulated with TNF-α, while solid gray histograms represent untreated controls.

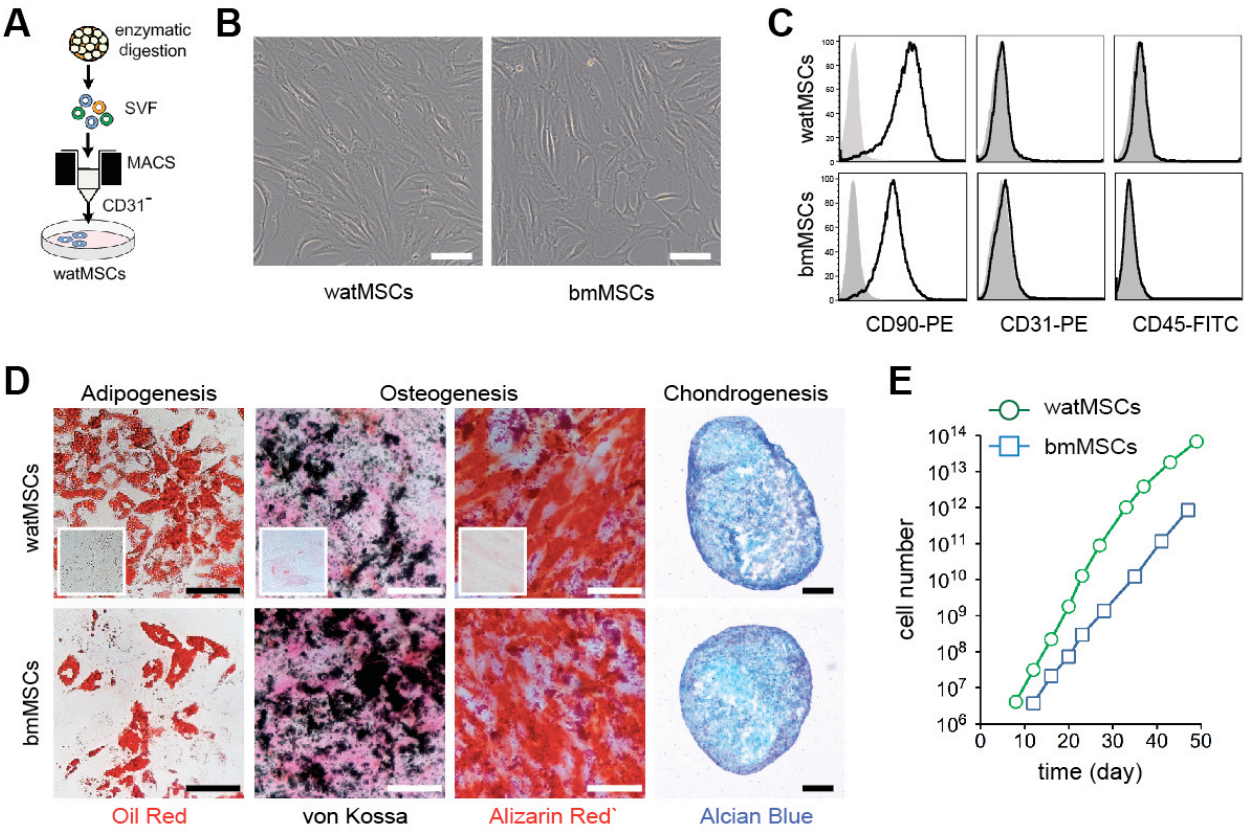


**Supplemental Figure 2. Isolation and culture expansion of MSCs from human WAT.** (A) Human watMSCs were isolated from subcutaneous WAT after enzymatic digestion and were selected as CD31- cells from the stromal vascular fraction (SVF). (B) Phase contrast micrographs of watMSCs and bmMSCs with characteristic spindle-shape morphology (scale bar: 100 µm). (C) Flow cytometry analysis of watMSCs and bmMSCs for CD31, CD90, and CD45. Black line histograms represent cells stained with fluorescent antibodies. Isotype-matched controls are overlaid in solid gray histograms. (D) Multilineage differentiation of MSCs in vitro. Differentiation into adipocytes was revealed by oil red O staining (scale bar 100 µm). Differentiation into osteocytes was revealed by Alizarin Red staining and von Kossa staining for calcium deposition and mineralization (scale bar 100 µm). Insets represent MSCs in non-differentiating control medium. Chondrogenic differentiation was revealed in pellet culture by the presence of glycosaminoglycans, detected by Alcian blue staining (scale bar 200 µm). (E) Expansion potential of watMSCs and bmMSCs measured by accumulative cell number in serially passaged cells.

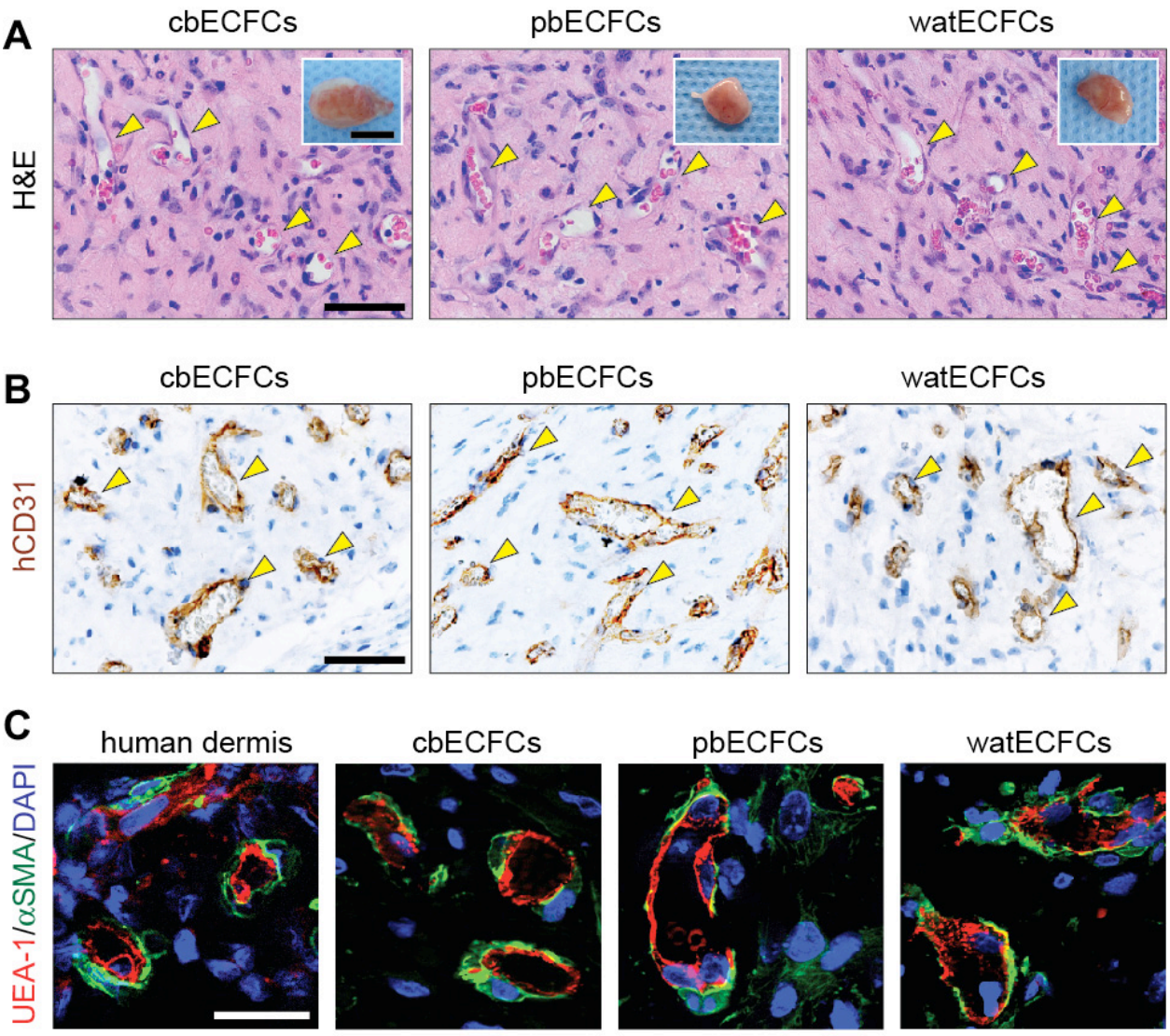


**Supplemental Figure 3. In vivo vasculogenic potential.** ECFCs were combined with MSCs and the mixture subcutaneously injected into nude mice (n=4) using collagen/fibrin-based gel. (A) H&E at day 8 from representative ECFC explants with numerous blood vessels containing RBCs (yellow arrowheads; scale bar: 50 μm). Inset represent the macroscopic views of the explants (scale bar: 5 mm). (B) hCD31 immunohistochemistry showed human specific lumens (yellow arrowheads; scale bars: 50 μm). (C) Perivascular coverage was assessed by double immunofluorescent staining of explants with UEA-1 (red) and α-SMA (green). Images are representative of all ECFC explants. Nuclei were counterstained with DAPI (scale bars: 50 μm).

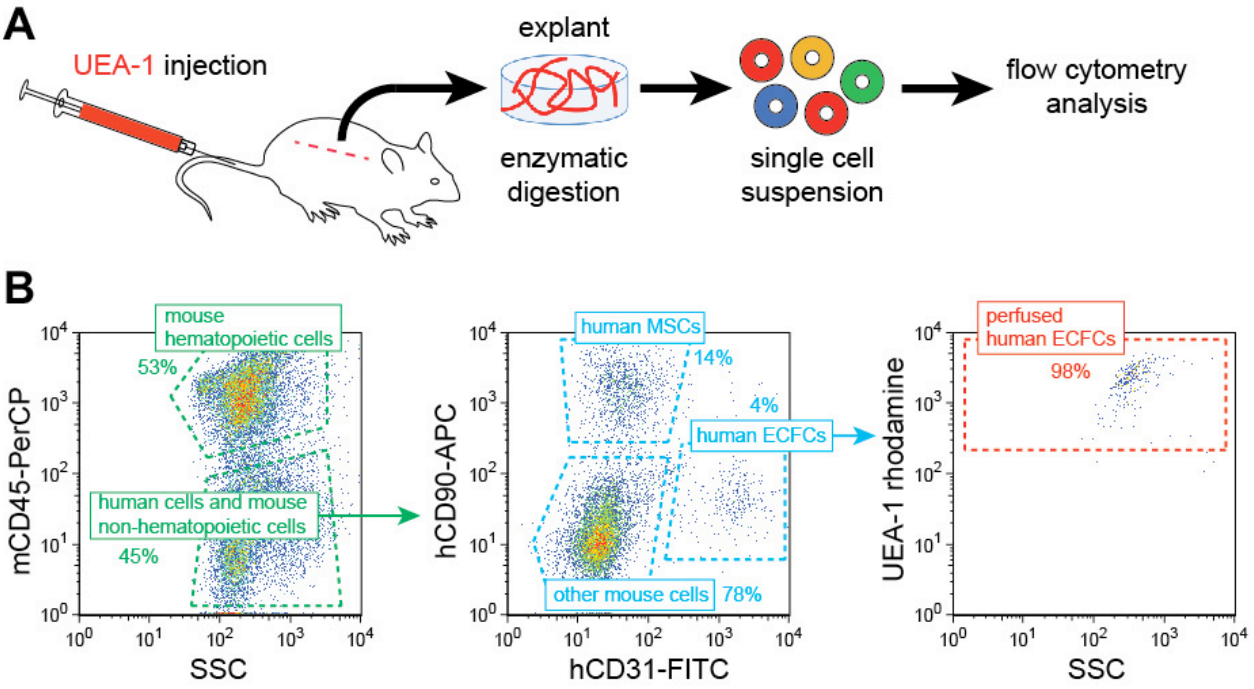


**Supplemental Figure 4. Quantification of lumenal ECFC engraftment by UEA-1 injection and FACS.** (A) Schematic diagram. To quantify lumenal engraftment, ECFCs/MSCs were implanted into nude mice. After 8 days, rhodamine-conjugated UEA-1 was injected (i.v.). and 10 min later the implants were excised and enzymatically digested. The number of ECFCs that were part of a perfused lumen ($hCD31^+/UEA\text{-}1^+$) was quantified by FACS. (B) FACS gating strategy. Human ECFCs ($mCD45^-/hCD90^{low}/hCD31^+$) were analyzed for rhodamine-conjugated UEA-1 binding. $hCD31^+/UEA\text{-}1^+$ cells were identified as perfused human ECFCs. Human MSCs ($mCD45^-/hCD90^{high}/hCD31^-$) served as negative binding control.